



Available online at www.sciencedirect.com

SCIENCE @ DIRECT®

Journal of Contaminant Hydrology 83 (2006) 1–26

JOURNAL OF
**Contaminant
Hydrology**
www.elsevier.com/locate/jconhyd

Steam stripping of the unsaturated zone of contaminated sub-soils: The effect of diffusion/dispersion in the start-up phase

H.J.H. Brouwers^a, B.H. Gilding^{b,*}

^a Department of Construction Technology, Faculty of Engineering Technology, University of Twente, P.O. Box 217, 7500 AE Enschede, The Netherlands

^b Department of Mathematics and Statistics, College of Science, Sultan Qaboos University, P.O. Box 36, Al-Khodh 123, Oman

Received 22 March 2004; received in revised form 5 September 2005; accepted 9 September 2005

Available online 15 December 2005

Abstract

The unsteady process of steam stripping of the unsaturated zone of soils contaminated with volatile organic compounds (VOCs) is addressed. A model is presented. It accounts for the effects of water and contaminants remaining in vapour phase, as well as diffusion and dispersion of contaminants in this phase. The model has two components. The first is a one-dimensional description of the propagation of a steam front in the start-up phase. This is based on Darcy's law and conservation laws of mass and energy. The second component describes the transport of volatile contaminants. Taking the view that non-equilibrium between liquid and vapour phases exists, it accounts for evaporation, transport, and condensation at the front. This leads to a moving-boundary problem. The moving-boundary problem is brought into a fixed domain by a suitable transformation of the governing partial differential equations, and solved numerically. For a broad range of the governing dimensionless numbers, such as the Henry, Merkel and Péclet numbers, computational results are discussed. A mathematical asymptotic analysis supports this discussion. The range of parameter values for which the model is valid is investigated. Diffusion and dispersion are shown to be of qualitative importance, but to have little quantitative effect in the start-up phase.

© 2005 Elsevier B.V. All rights reserved.

Keywords: Steam stripping; Contaminant; VOC; Unsaturated zone; Start-up; Model; Diffusion; Dispersion

* Corresponding author. Tel.: +968 24141430; fax: +968 24415490.

E-mail addresses: h.j.h.brouwers@utwente.nl (H.J.H. Brouwers), gilding@squ.edu.om (B.H. Gilding).

Notation		<i>Greek letters</i>	
<i>Roman letters</i>		β parameter	
A	parameter [$m^2 s^{-1}$]	γ parameter	
a	coefficient in discretized equation	ε parameter	
b	coefficient in discretized equation	η boundary-layer variable	
C	contaminant concentration [$kg m^{-3}$]	κ effective permeability [m^2]	
C_{lm}	solubility [$kg m^{-3}$]	λ parameter	
c	coefficient in discretized equation	ν kinematic viscosity [$m^2 s^{-1}$]	
c_p	specific heat [$J kg^{-1} K^{-1}$]	ξ dimensionless spatial variable	
D	binary diffusion coefficient [$m^2 s^{-1}$]	ρ density [$kg m^{-3}$]	
f	known vector in discretized equation	τ dimensionless time variable	
g_t	mass-transfer coefficient [s^{-1}]	ϕ porosity	
H	Henry's law coefficient	<i>Subscripts</i>	
H_{lat}	latent heat of condensation [$J kg^{-1}$]	air	pertaining to displaced fluid
h	size of discretization step	c	condensate
i	counter	i	index
K	thermal conductivity [$W m^{-1} K^{-1}$]	in	injection
k	counter	k	index
L	distance from injection to monitoring point [m]	l	pertaining to liquid phase
M	Merkel number	s	pertaining to solid
m	molecular mass of contaminant [$kg mol^{-1}$]	sat	saturation
n	number of discretization steps	v	pertaining to vapour phase
P	Péclet number	0	pertaining to initial condition
p	pressure [Pa]	<i>Superscripts</i>	
R	gas constant [$J K^{-1} mol^{-1}$]	i	index
S	saturation	k	index
T	temperature [K]	(0)	leading term
t	time [s]	(1)	second to leading term
u	velocity [$m s^{-1}$]	—	mean
X	position of steam front [m]	~	transformed
x	coordinate [m]	*	limit
		~	boundary-layer

1. Introduction

Steam flow in porous media with heat transfer and condensation is encountered in many practical applications. Examples are enhanced oil recovery by steam injection, geothermal energy production, drying processes, and cleaning soils contaminated with organic compounds. For an overview of previous experimental and theoretical work on steam stripping of soils, see (Brouwers, 1996; van der Ham and Brouwers, 1998; Brouwers and Augustijn, 2001) and the references therein.

The start-up phase of steam stripping has previously been studied in publications of Brouwers and Li (1994, 1995). The liquid contaminant concentration is assumed to be below the solubility limit of the interstitial water (no free VOC). The non-equilibrium transfer of

sorbed/dissolved VOC is included by using Henry's law. A limitation of these previous studies is that the mass of vapour is assumed to be negligible when compared to the mass of condensed water. Another limitation is that the effect of diffusion and dispersion is ignored. Nonetheless, the latter mode of transport is likely to be relevant when the advective transport of contaminant is relatively small.

The present paper extends the previous studies of the start-up phase of the steam stripping process. In improvement on the earlier studies, here the mass of vapour behind the steam front is not neglected, and, diffusion/dispersion of the contaminant in the steam phase is retained. Analogous to [Brouwers and Li \(1995\)](#), a one-dimensional situation is considered. This is useful for interpreting column experiments and for verifying more complicated numerical models.

2. Steam flow

This section recapitulates and extends the model of the one-dimensional and unsteady propagation of a steam front in soil of [Brouwers and Li \(1994, 1995\)](#). The soil is considered as a homogeneous and isotropic porous medium. The process involves the displacement of air by water-vapour, with condensation of the water-vapour and release of latent heat. This heat is used to warm up the soil and the initially resident groundwater.

The steam is injected at $x=0$ at a constant pressure p_{in} . The steam flows through the unsaturated matrix to the condensation front, whose position at the time t is designated by $X(t)$, where the ambient pressure p_0 prevails ([Fig. 1](#)). Condensation occurs at the front until the soil and the initial groundwater are heated up to the saturation temperature T_{sat} of the steam. The pressure drop between injection point and condensation front (typically 10^4 Pa) is much smaller than the absolute pressure in the porous medium (ambient pressure). So T_{sat} may be regarded as constant. Hence, behind the steam front ($0 \leq x \leq X(t)$, $t > 0$), the temperature of the mixture of soil, water and steam equals this value.

Assuming that the vapour displaces the air evenly, the liquid phase is immobile (i.e. the water saturation is smaller than irreducible water saturation) and that the resistance to vapour flow is much larger than to air flow, the steam flow to the front obeys Darcy's law

$$u_v \rho_v = \frac{\kappa}{v_v} \frac{p_{\text{in}} - p_0}{X}, \quad (1)$$

where u_v denotes the velocity of the injected vapour, ρ_v its density, κ the effective permeability of the soil with respect to the vapour, and v_v the kinematic viscosity of the vapour mix.

Let ϕ denote the porosity of the soil, S_{10} the initial saturation of the water, S_{air} the saturation of the air, S_v the saturation of the vapour, and S_{lc} the saturation of the condensation water. So,

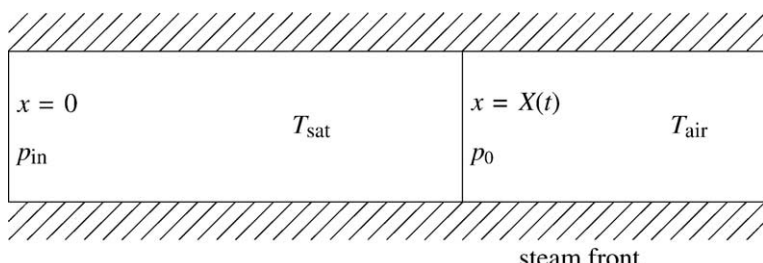


Fig. 1. Schematic representation of process.

initially and ahead of the front,

$$S_{l0} + S_{air} = 1,$$

while, behind the front,

$$S_{l0} + S_{lc} + S_v = 1.$$

A mass balance of injected water vapour, accumulated condensate and water vapour behind the front, yields

$$u_v \rho_v = \phi(\rho_l S_{lc} + \rho_v S_v) \frac{dX}{dt}, \quad (2)$$

where ρ_l denotes the density of the condensation water. A similar mass balance ahead of the front gives

$$u_{air} = \phi S_{air} \frac{dX}{dt}, \quad (3)$$

in which u_{air} is the velocity of the displaced air.

In their original model, [Brouwers and Li \(1994, 1995\)](#) assumed that the flow is condensation dominated, i.e.

$$\varepsilon = \frac{\rho_v S_v}{\rho_l S_{lc}} \ll 1. \quad (4)$$

This is justified if the amount of condensed water is much larger than the amount of vapour in the pores. In the present paper assuming merely that ε is constant, an analysis analogous to the case that ε is negligible will be executed.

Ahead of the front ($x > X(t)$, $t > 0$), the temperature of soil and its constituents, T_{air} , satisfies the energy equation

$$\overline{\rho_s c_{ps}} \frac{\partial T_{air}}{\partial t} = \overline{K_s} \frac{\partial^2 T_{air}}{\partial x^2}, \quad (5)$$

where $\overline{K_s}$ and $\overline{\rho_s c_{ps}}$ represent the thermal conductivity and heat capacity of the soil and its constituents, respectively. Initially, the temperature has a uniform value T_0 , i.e.

$$T_{air}|_{t=0} = T_0. \quad (6)$$

At all later times at the front,

$$T_{air}|_{x=X} = T_{sat}. \quad (7)$$

Also from an analysis of the liberated energy,

$$-\overline{K_s} \frac{\partial T_{air}}{\partial x} \Big|_{x=X} = \phi \rho_l S_{lc} H_{lat} \frac{dX}{dt}, \quad (8)$$

where H_{lat} denotes the latent heat of condensation. Combining Eqs. (1) and (2), the above condition can be written as

$$-\overline{K_s} \frac{\partial T_{air}}{\partial x} \Big|_{x=X} = \frac{\kappa H_{lat}(p_{in} - p_0)}{(1 + \varepsilon)v_v X}. \quad (9)$$

Subsequently, defining

$$A = \frac{2\kappa H_{\text{lat}}(p_{\text{in}} - p_0)}{\nu_v \rho_s c_{\text{ps}} (T_{\text{sat}} - T_0)}$$

and

$$\gamma = \sqrt{\frac{\kappa H_{\text{lat}}(p_{\text{in}} - p_0)}{2(1+\varepsilon)\nu_v \bar{K}_s (T_{\text{sat}} - T_0)}}, \quad (10)$$

it can be verified that the solution of problem (5)–(7), (9) is given by

$$X(t) = \lambda \sqrt{\frac{At}{1+\varepsilon}} \quad \text{and} \quad (11)$$

$$T_{\text{air}}(x, t) = T_0 + (T_{\text{sat}} - T_0) \frac{\operatorname{erfc}(\gamma \lambda x / X(t))}{\operatorname{erfc}(\gamma \lambda)}, \quad (12)$$

where erfc denotes the complementary error function, i.e.

$$\operatorname{erfc}(z) = \frac{2}{\sqrt{\pi}} \int_z^\infty \exp(-s^2) ds,$$

and λ follows from the equation

$$\sqrt{\pi}\gamma \exp(\gamma^2 \lambda^2) \operatorname{erfc}(\gamma \lambda) = \lambda. \quad (13)$$

For a given γ , λ can be determined as the root of Eq. (13). Numerical computations using the bisection method were presented by Brouwers and Li (1994, 1995). Explicit functions that give a good approximation were given by Brouwers and Li (1994) and Gilding and Li (1997). In particular, Gilding and Li (1997) proposed an explicit function that determines $\lambda(\gamma)$ with a relative error of less than 0.4%. A plot of this function is displayed in Fig. 2. For a more detailed study of Eq. (13) the reader is referred to the papers of Gilding and Li (1997) and Russo (1998).

Substituting expressions (11) and (12) in (8) gives

$$\rho_l S_{lc} = \frac{\overline{\rho_s c_{ps}} (T_{\text{sat}} - T_0)}{\lambda^2 \phi H_{\text{lat}}}.$$

This identity confirms that also in the case that $\varepsilon > 0$ the amount of condensed steam does not depend on the position of the front. Hence, the water saturation behind the front is constant. Furthermore, the effective permeability κ , which in general depends on S_l , is also constant. In

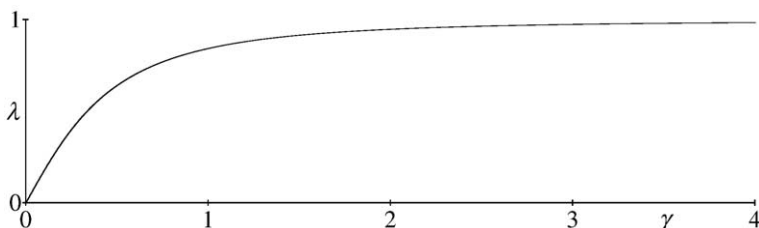


Fig. 2. The parameter λ as a function of γ .

contrast to in the analysis of Brouwers and Li (1994, 1995), S_{lc} now has to be determined iteratively as λ depends on ε (see formulae (10) and (13)), while ε in turns depends on S_{lc} (see formula (4)). However, the form of λ as a function of γ is such that successive substitution with a starting value of $\varepsilon=0$ will lead to a bracketing of the actual value of S_{lc} . The latter can subsequently easily be determined by standard root-finding techniques such as those presented by Press et al. (1986). Thus the analysis in the case that ε is assumed to be negligible, extends to the case that ε is assumed to be constant but not necessarily equal to zero.

An experimental study of constant-pressure steam injection in a sand column is reported by Brouwers (1996). The conditions in this study are such that the parameter γ defined by (10) ranges from 40 to 47. The study shows that the transient position of the steam front predicted with the present model is in good agreement with experimental observation.

3. Contaminant transport

A common assumption made in the chemical engineering field is that the mass transfer of contaminant between liquid and vapour phases is proportional to the deviation from equilibrium. In other words, if C_l denotes the concentration in the liquid phase and C_v the concentration in vapour phase, the transfer is given by $g_t(HC_l - C_v)$ where g_t is a mass-transfer coefficient and H is a dimensionless Henry's law coefficient. The latter reflects the contaminant pressure p_{sat} at the temperature T_{sat} , the molecular mass m of the contaminant, the gas constant R , and the solubility of the contaminant C_{lm} , via the formula $H = mp_{sat}/RT_{sat}C_{lm}$.

For the vapour phase, a differential mass balance gives

$$\phi S_v \frac{\partial C_v}{\partial t} = D \frac{\partial^2 C_v}{\partial x^2} - u_v \frac{\partial C_v}{\partial x} + g_t(HC_l - C_v), \quad (14)$$

where D is the coefficient of diffusion/dispersion. This formulation differs from that of Brouwers and Li (1995) in that it includes diffusion and dispersion.

The mass balance of the contaminant in the water phase is governed by

$$\phi(S_{l0} + S_{lc}) \frac{\partial C_l}{\partial t} = -g_t(HC_l - C_v). \quad (15)$$

Eq. (15) does not explicitly include sorption. However, Eqs. (14) and (15) with different coefficients can still be considered as an appropriate model if linear sorption is assumed (Brouwers, 1999).

Eqs. (14) and (15) are valid in the domain $t > 0$ and $0 < x < X(t)$ (Fig. 3). In order to form a well-posed problem and solve Eqs. (14) and (15), boundary conditions have to be specified. At the entrance, i.e. $x = 0$, the zero flux condition reads

$$\left(u_v C_v - D \frac{\partial C_v}{\partial x} \right) \Big|_{x=0} = 0. \quad (16)$$

Further boundary conditions at the front can be obtained by considering local mass balances.

Suppose that the concentration of the contaminant in the air ahead of the steam front is C_{air} . Then the passage of the front results in a change in contaminant mass at a rate of $\phi(S_v C_v - S_{air} C_{air}) \frac{dX}{dt}$. In addition, water condenses at a rate of $\phi \rho_l S_{lc} \frac{dX}{dt}$ at the front. This gives rise to transfer of contaminant from the vapour phase into the condensation water at the front at a rate of $\phi(\rho_l / \rho_v) S_{lc} C_v \frac{dX}{dt}$. Hence, noting that ahead of the front the contaminant flux is

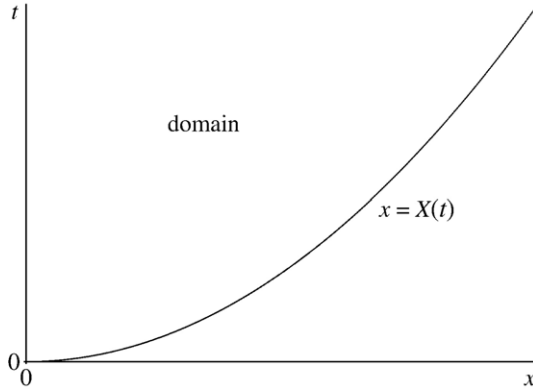


Fig. 3. Domain of moving-boundary problem.

$u_{\text{air}}C_{\text{air}}$, conservation of mass requires that

$$\left(u_v C_v - D \frac{\partial C_v}{\partial x} \right) \Big|_{x=X} = \phi (S_v C_v|_{x=X} - S_{\text{air}} C_{\text{air}}) \frac{dX}{dt} + \phi \frac{\rho_l}{\rho_v} S_{\text{lc}} C_v \Big|_{x=X} \frac{dX}{dt} + u_{\text{air}} C_{\text{air}}. \quad (17)$$

Using expressions (2) and (3) to eliminate u_v and u_{air} from this local balance gives the boundary condition

$$D \frac{\partial C_v}{\partial x} \Big|_{x=X} = 0. \quad (18)$$

A similar mass balance can be made for the contaminant in the liquid phase. Suppose that the initial concentration of the contaminant in the liquid phase is C_{l0} . Then the passage of the front results in a change of contaminant mass at a rate of $\phi \{(S_{l0} + S_{\text{lc}})C_l - S_{l0}C_{l0}\} \frac{dX}{dt}$. While, from previous deduction, there is mass transfer to the liquid phase at a rate $\phi(\rho_l/\rho_v)S_{\text{lc}}C_v \frac{dX}{dt}$. Subsequently, by conservation of mass in the liquid phase at the front there must hold

$$\phi \{(S_{l0} + S_{\text{lc}})C_l|_{x=X} - S_{l0}C_{l0}\} \frac{dX}{dt} = \phi \frac{\rho_l}{\rho_v} S_{\text{lc}} C_v|_{x=X} \frac{dX}{dt}. \quad (19)$$

Simplifying this expression leads to the boundary condition

$$\left(C_l - \frac{\rho_l S_{\text{lc}}}{\rho_v (S_{l0} + S_{\text{lc}})} C_v \right) \Big|_{x=X} = \frac{S_{l0}}{S_{l0} + S_{\text{lc}}} C_{l0}. \quad (20)$$

In comparison with the analysis of [Brouwers and Li \(1995\)](#) the presented model accounts for diffusion/dispersion and for a non-negligible saturation of vapour phase S_v .

Conditions (17) and (19), and therefore (18) and (20) can also be derived as macroscopic boundary conditions following the treatment of such conditions in ([Bear, 1979](#)). Note that addition of Eqs. (14) and (15), integration and substitution of the boundary conditions (16), (18) and (20) leads to the identity

$$\int_0^{X(t)} \phi \{S_v C_v + (S_{l0} + S_{\text{lc}})C_l\} dx = \phi S_{l0} C_{l0} X(t) \quad (21)$$

for every $t \geq 0$. This is the statement of an overall conservation of mass.

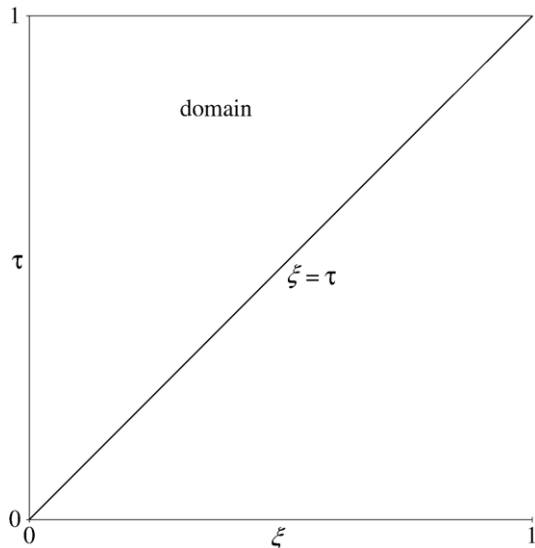


Fig. 4. Domain of moving-boundary problem in dimensionless coordinates.

Bearing in mind that no free VOC is envisaged, a constraint imposed on the viability of the above model is that the liquid contaminant concentration does not exceed the solubility limit, i.e.

$$C_l \leq C_{lm}. \quad (22)$$

Correspondingly,

$$C_v \leq H C_{lm}. \quad (23)$$

If the solubility limit is exceeded, free VOC is created. For such a situation, alternative models, which have been validated by experiments, are available (van der Ham and Brouwers, 1998; Brouwers and Augustijn, 2001). The possibility of this precipitation of non-aqueous phase liquid (NAPL) is typical of the transient process studied here. In general this formation is undesirable, as dense NAPL (DNAPL) may migrate under the influence of gravity, thus further impeding the remedial action of the steam stripping.

The independent variables in Eqs. (14) and (15) and boundary conditions (16), (18) and (20) can be made dimensionless by defining

$$\xi = \frac{x}{L} \quad \text{and} \quad \tau = \frac{X(t)}{L},$$

where L represents the distance between the injection point and some monitoring point for instance. In terms of these variables, the position of the front is given by $\xi = \tau$, and, the front will arrive at the monitoring point at $\tau = 1$ (Fig. 4). The dependent variables can be made dimensionless by defining

$$\tilde{C}_v = \frac{\rho_l C_v}{\rho_v C_{lm}} \quad \text{and} \quad \tilde{C}_l = \frac{C_l}{C_{lm}}.$$

Together, this transforms problem (14)–(16) into the equations

$$\frac{\varepsilon}{1+\varepsilon} \frac{\partial \tilde{C}_v}{\partial \tau} = \frac{\tau}{P} \frac{\partial^2 \tilde{C}_v}{\partial \xi^2} - \frac{\partial \tilde{C}_v}{\partial \xi} + M\tau(\tilde{H}\tilde{C}_1 - \tilde{C}_v) \quad (24)$$

and

$$\frac{\partial \tilde{C}_1}{\partial \tau} = -\beta(1+\varepsilon)M\tau(\tilde{H}\tilde{C}_1 - \tilde{C}_v) \quad (25)$$

for $0 < \xi < \tau \leq 1$, with the boundary conditions

$$\left(\tilde{C}_v - \frac{\tau}{P} \frac{\partial \tilde{C}_v}{\partial \xi} \right) \Big|_{\xi=0} = 0, \quad (26)$$

$$\frac{1}{P} \frac{\partial \tilde{C}_v}{\partial \xi} \Big|_{\xi=\tau} = 0, \quad (27)$$

and

$$(\tilde{C}_1 - \beta \tilde{C}_v) \Big|_{\xi=\tau} = (1-\beta)\tilde{C}_{10} \quad (28)$$

for $0 < \tau \leq 1$. In the above

$$P = \frac{\kappa(p_{in} - p_0)}{\rho_v v_v D}$$

represents the Péclet number which constitutes a ratio of advective transport to diffusion/dispersion,

$$M = \frac{\rho_v v_v g_t L^2}{\kappa(p_{in} - p_0)}$$

represents the dimensionless Merkel number constituting a ratio between the mass-transfer rate and transport rate,

$$\tilde{H} = \frac{\rho_l}{\rho_v} H$$

represents the transformed Henry number,

$$\beta = \frac{S_{lc}}{S_{l0} + S_{lc}}$$

the ratio of the amount of condensation water to the water saturation after the passage of the front, and,

$$\tilde{C}_{10} = \frac{C_{10}}{C_{lm}}$$

the dimensionless initial concentration of contaminant in the liquid phase. Expressed in the new variables, the physical constraints (22) and (23) become respectively

$$\tilde{C}_1 \leq 1 \quad (29)$$

and

$$\tilde{C}_v \leq \tilde{H}. \quad (30)$$

Together (24)–(28) form a well-posed boundary-value problem. Moreover, in the limiting case $P=\infty$, Eq. (24) reduces to a first-order partial differential equation, the boundary condition (26) becomes simply $\tilde{C}_v|_{\xi=0}=0$, while (27) is satisfied vacuously. So that in this case too, the problem is well-posed. This limiting case corresponds to diffusion/dispersion being neglected. When moreover $\varepsilon=0$, i.e. saturation in vapour phase is neglected, the system reduces further to precisely that analyzed by [Brouwers and Li \(1995\)](#).

In terms of the transformed variables, the statement of overall conservation of mass (21) becomes

$$\int_0^\tau \{\beta\varepsilon\tilde{C}_v(\xi, \tau) + \tilde{C}_l(\xi, \tau)\} d\xi = (1-\beta)\tilde{C}_{l0}\tau \quad (31)$$

for $0 < \tau \leq 1$. Successively differentiating this identity with respect to τ , using Eqs. (24) and (25) to eliminate $\partial\tilde{C}_v/\partial\tau$ and $\partial\tilde{C}_l/\partial\tau$, respectively, evaluating the remaining integral and incorporating (26) leads to the relation

$$\left. \left(\beta(1+\varepsilon) \frac{\tau}{P} \frac{\partial\tilde{C}_v}{\partial\varepsilon} + \tilde{C}_l - \beta\tilde{C}_v \right) \right|_{\xi=\tau} = (1-\beta)\tilde{C}_{l0} \quad (32)$$

for $0 < \tau \leq 1$. This relation may therefore be viewed as the boundary condition that is essential for overall mass conservation. In fact, retracing the above argument, it can be seen to be fully equivalent to (31). Relation (32) follows from (27) and (28). However, the converse cannot be said.

4. Qualitative influence of parameters

A numerical scheme has been developed to solve the boundary-value problem derived in the previous section. Details of this scheme, together with a description of its validation, are presented as an appendix. As part of the validation, the numerical scheme has been shown to be capable of reproducing the results, neglecting the retention of water in the vapour phase ($\varepsilon=0$) and diffusion/dispersion ($P=\infty$), obtained previously by [Brouwers and Li \(1995\)](#). A value of $P=10^{99}$ was used to emulate $P=\infty$. This section describes the confirmation that the effect of the two new aspects considered in the present paper, i.e. accounting for the retention of water in the vapour phase ($\varepsilon>0$) and for diffusion/dispersion ($P<\infty$), has the phenomenological effects that one would expect.

For the purpose of investigating the influence of diffusion/dispersion, computations were carried out with the representative parameter values $\tilde{C}_{l0}=0.25$, $\beta=0.5$, $M=0.1$, $\tilde{H}=40$ and $\varepsilon=0$. Profiles of the computed dimensionless concentrations \tilde{C}_l and \tilde{C}_v as functions of the dimensionless coordinate ξ at the end of the process, i.e. for $\tau=1$, were examined. Decreasing the Péclet number from 10^{99} to 100 did not result in any significant change in the profiles. Nevertheless, for smaller Péclet numbers there is an effect which can be seen in [Fig. 5](#). In this figure, it can be seen that variation of the Péclet number involves no significant alteration of the dimensionless concentration in the liquid phase \tilde{C}_l . However, decreasing the Péclet number does result in a redistribution of the dimensionless concentration in the vapour phase \tilde{C}_v , whereby the profile displays a greater uniformity with larger concentrations far from the front at the expense

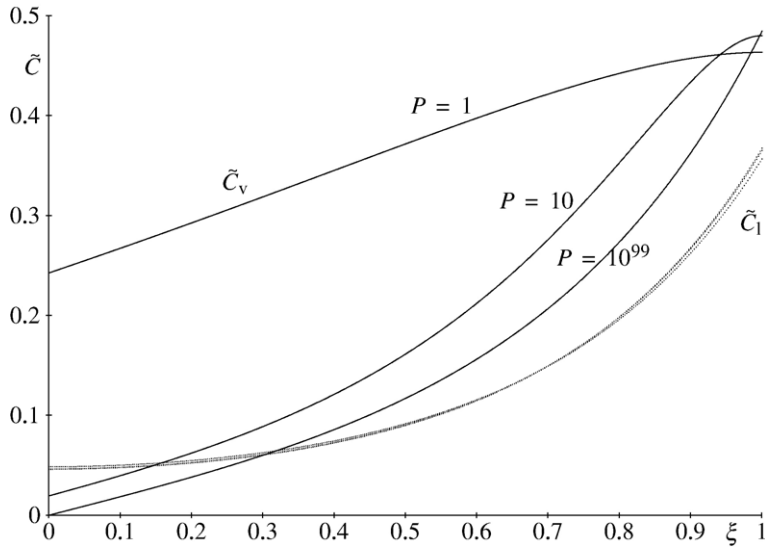


Fig. 5. Profiles showing the qualitative effect of the size of the Péclet number P .

of those nearer the front. Both of these observations are consistent with a physical increase of diffusion/dispersion.

Retaining the parameter values $\tilde{C}_{10}=0.25$, $\beta=0.5$, $M=0.1$ and $\tilde{H}=40$ together with $P=1$, and the previous profiles, the effect of subsequently altering the value of ε is shown in Fig. 6. One sees that increasing ε has the effect of decreasing the dimensionless concentrations in both the vapour and liquid phases. This is compatible with the observation that, all other things being equal, from the total mass balance (31) it follows that increasing ε has to result somewhere in a decrease of \tilde{C}_v , \tilde{C}_l , or both.

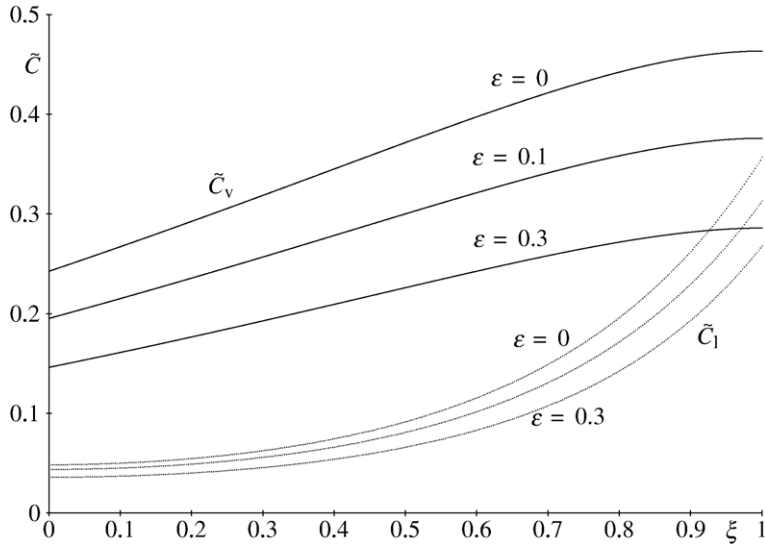


Fig. 6. Profiles showing the qualitative effect of the size of the parameter ε .

From further numerical experiments, it appears that at a small Merkel number ($M=10^{-3}$) which leads to low concentrations, changing the value of ε has little influence on the final process. This is in contrast to when $M=0.1$, in which case the dimensionless concentrations are larger, and increasing ε from 0 to 0.3 results in a noticeable decrease of the concentration of contaminant in vapour phase. In particular, for $\tilde{C}_{10}=0.25$, $\beta=0.5$, $M=0.1$, $\tilde{H}=400$ and $P=1$, this can result in a reduction of 79%.

5. Asymptotic analysis

As is reported in the next section, where the influence of diffusion/dispersion on the start-up phase of steam stripping of contaminated soil will be quantitatively analyzed using the numerical model, in practice the Henry number can vary three orders of magnitude, while the Merkel number can vary up to no less than ten orders. This can result in strongly contrasting behaviour. One phenomenon previously revealed by the computations of Brouwers and Li (1995) is that the simulated dimensionless liquid contaminant concentration may not comply to the physical constraint (29). In this section, in preparation to the discussion of the quantitative analysis including satisfaction of both the physical constraints (29) and (30), the limiting behaviour will be deduced analytically.

Case 1 (*Vanishing Merkel number; i.e. $M \rightarrow 0$*). The limiting situation $M \rightarrow 0$ is amenable to regular perturbation analysis. Substituting $\tilde{C}_v = \tilde{C}_v^{(0)}(\xi, \tau) + O(M)$ and $\tilde{C}_l = \tilde{C}_l^{(0)}(\xi, \tau) + O(M)$ in problem (24)–(28), and collecting terms of leading order in M yields

$$\frac{\varepsilon}{1+\varepsilon} \frac{\partial \tilde{C}_v^{(0)}}{\partial \tau} = \frac{\tau}{P} \frac{\partial^2 \tilde{C}_v^{(0)}}{\partial \xi^2} - \frac{\partial \tilde{C}_v^{(0)}}{\partial \xi} \quad (33)$$

and

$$\frac{\partial \tilde{C}_l^{(0)}}{\partial \tau} = 0$$

for $0 < \xi < \tau \leq 1$ together with the boundary conditions (26)–(28) for $0 < \tau \leq 1$ with $\tilde{C}_v^{(0)}$ and $\tilde{C}_l^{(0)}$ in lieu of \tilde{C}_v and \tilde{C}_l , respectively. It is easily recognizable that

$$\tilde{C}_v^{(0)} \equiv 0 \quad \text{and} \quad \tilde{C}_l^{(0)} \equiv (1-\beta)\tilde{C}_{10} \quad (34)$$

is the only plausible solution to this problem. Thus in the limit $M \rightarrow 0$, one can determine that

$$\tilde{C}_v(\xi, \tau) = O(M) \quad \text{and} \quad \tilde{C}_l(\xi, \tau) = (1-\beta)\tilde{C}_{10} + O(M).$$

Note that $\tilde{C}_v \equiv 0$ and $\tilde{C}_l \equiv (1-\beta)\tilde{C}_{10}$ satisfies the overall mass-balance identity (31).

Case 2 (*Vanishing Henry number; i.e. $\tilde{H} \rightarrow 0$*). The limit $\tilde{H} \rightarrow 0$ can be treated like the previous case. Setting $\tilde{C}_v = \tilde{C}_v^{(0)}(\xi, \tau) + O(\tilde{H})$ and $\tilde{C}_l = \tilde{C}_l^{(0)}(\xi, \tau) + O(\tilde{H})$, in the limit $\tilde{H} \rightarrow 0$ Eqs. (24) and (25) become

$$\frac{\varepsilon}{1+\varepsilon} \frac{\partial \tilde{C}_v^{(0)}}{\partial \tau} = \frac{\tau}{P} \frac{\partial^2 \tilde{C}_v^{(0)}}{\partial \xi^2} - \frac{\partial \tilde{C}_v^{(0)}}{\partial \xi} - M\tau\tilde{C}_v^{(0)}$$

and

$$\frac{\partial \tilde{C}_l^{(0)}}{\partial \tau} = \beta(1+\varepsilon)M\tau\tilde{C}_v^{(0)}$$

for $0 < \xi < \tau \leq 1$, while the boundary conditions (26)–(28) with $\tilde{C}_v^{(0)}$ and $\tilde{C}_l^{(0)}$ in lieu of \tilde{C}_v and \tilde{C}_l , respectively, remain applicable. Although not quite as obvious as in the previous case, it is nonetheless verifiable that (34) also solves this problem. Thus, as $\tilde{H} \rightarrow 0$, one finds

$$\tilde{C}_v(\xi, \tau) = O(\tilde{H}) \quad \text{and} \quad \tilde{C}_l(\xi, \tau) = (1 - \beta)\tilde{C}_{l0} + O(\tilde{H}).$$

It transpires then in both the cases that the Merkel number or the Henry number vanishes, the limiting situation is one in which there is no contaminant in the vapour phase while the contaminant remains uniformly distributed in liquid phase behind the steam front. This is precisely what one would physically expect.

Case 3 ($M \rightarrow \infty$). In contrast to the previous two cases, the limit $M \rightarrow \infty$ leads to a singular perturbation problem. Substituting

$$\tilde{C}_v = \tilde{C}_v^{(0)}(\xi, \tau) + \tilde{C}_v^{(1)}(\xi, \tau)/M + O(1/M^2) \quad (35)$$

and

$$\tilde{C}_l = \tilde{C}_l^{(0)}(\xi, \tau) + \tilde{C}_l^{(1)}(\xi, \tau)/M + O(1/M^2) \quad (36)$$

in either Eq. (24) or Eq. (25), dividing by M , and then passing to the limit $M \rightarrow \infty$ yields

$$\tilde{C}_l^{(0)} \equiv \frac{\tilde{C}_v^{(0)}}{\tilde{H}}. \quad (37)$$

Insertion of (35)–(37) in Eqs. (24) and (25) gives

$$\frac{\varepsilon}{1 + \varepsilon} \frac{\partial \tilde{C}_v^{(0)}}{\partial \tau} = \frac{\tau}{P} \frac{\partial^2 \tilde{C}_v^{(0)}}{\partial \xi^2} - \frac{\partial \tilde{C}_v^{(0)}}{\partial \xi} + \tau \left(\tilde{H} \tilde{C}_l^{(1)} - \tilde{C}_v^{(1)} \right)$$

and

$$\frac{1}{\tilde{H}} \frac{\partial \tilde{C}_v^{(0)}}{\partial \tau} = -\beta(1 + \varepsilon)\tau \left(\tilde{H} \tilde{C}_l^{(1)} - \tilde{C}_v^{(1)} \right)$$

in the limit $M \rightarrow \infty$, respectively. From these two equations $\tilde{H} \tilde{C}_l^{(1)} - \tilde{C}_v^{(1)}$ may be eliminated, to deduce that necessarily

$$\frac{1 + \beta\varepsilon\tilde{H}}{\beta(1 + \varepsilon)\tilde{H}} \frac{\partial \tilde{C}_v^{(0)}}{\partial \tau} = \frac{\tau}{P} \frac{\partial^2 \tilde{C}_v^{(0)}}{\partial \xi^2} - \frac{\partial \tilde{C}_v^{(0)}}{\partial \xi} \quad (38)$$

for $0 < \xi < \tau \leq 1$. Simultaneously, insertion of (35)–(37) in (26)–(28) and passage to the limit $M \rightarrow \infty$ gives the boundary conditions

$$\left. \left(\tilde{C}_v^{(0)} - \frac{\tau}{P} \frac{\partial \tilde{C}_v^{(0)}}{\partial \xi} \right) \right|_{\xi=0} = 0, \quad (39)$$

$$\left. \frac{1}{P} \frac{\partial \tilde{C}_v^{(0)}}{\partial \xi} \right|_{\xi=\tau} = 0 \quad (40)$$

and

$$\left. \frac{1 - \beta\tilde{H}}{\tilde{H}} \tilde{C}_v^{(0)} \right|_{\xi=\tau} = (1 - \beta)\tilde{C}_{l0} \quad (41)$$

for $0 < \tau \leq 1$.

In general, (38)–(41) constitutes an over-determined system. The only exception is when $P=\infty$ and $\beta\tilde{H}<1$, in which case (38) becomes

$$\frac{1+\beta\varepsilon\tilde{H}}{\beta(1+\varepsilon)\tilde{H}} \frac{\partial\tilde{C}_v^{(0)}}{\partial\tau} + \frac{\partial\tilde{C}_v^{(0)}}{\partial\xi} = 0, \quad (42)$$

and, (39) and (40) reduce to

$$\tilde{C}_v^{(0)}|_{\xi=0} = 0 \quad (43)$$

for $0<\tau\leq 1$. Using the method of characteristics, it can be established that problem (41)–(43) admits the unique solution

$$\tilde{C}_v^{(0)}(\xi, \tau) = \begin{cases} 0 & \text{for } \xi < \frac{\beta(1+\varepsilon)\tilde{H}}{1+\beta\varepsilon\tilde{H}}\tau \\ \frac{(1-\beta)\tilde{H}}{1-\beta\tilde{H}}\tilde{C}_{10} & \text{for } \xi > \frac{\beta(1+\varepsilon)\tilde{H}}{1+\beta\varepsilon\tilde{H}}\tau. \end{cases} \quad (44)$$

Note that this implies that in the limit $M\rightarrow\infty$ the solution of the original problem (24)–(28) converges to a pair of discontinuous step-functions. Nonetheless these limiting functions, given by (37) and (44), do conform to the overall conservation of mass identity (31). See Fig. 7 for an illustration of the phenomenon by a numerically computed solution. The parameter values used in this computation are $\tilde{C}_{10}=0.25$, $\beta=0.5$, $M=10^5$, $\tilde{H}=0.1$, $\varepsilon=0$ and $P=10^{99}$. The figure shows the dimensionless concentration in the liquid phase \tilde{C}_l and in the vapour phase \tilde{C}_v as a function of ξ , for $\tau=1$.

When $P<\infty$, it is not possible to find a function that satisfies Eq. (38) and all three boundary conditions (39)–(41). This would suggest that in the limit $M\rightarrow\infty$, a discontinuity in the solution arises in such a manner that one of the boundary conditions is annihilated. To divine how this happens, note that first and foremost the principle of conservation of mass has to be preserved.

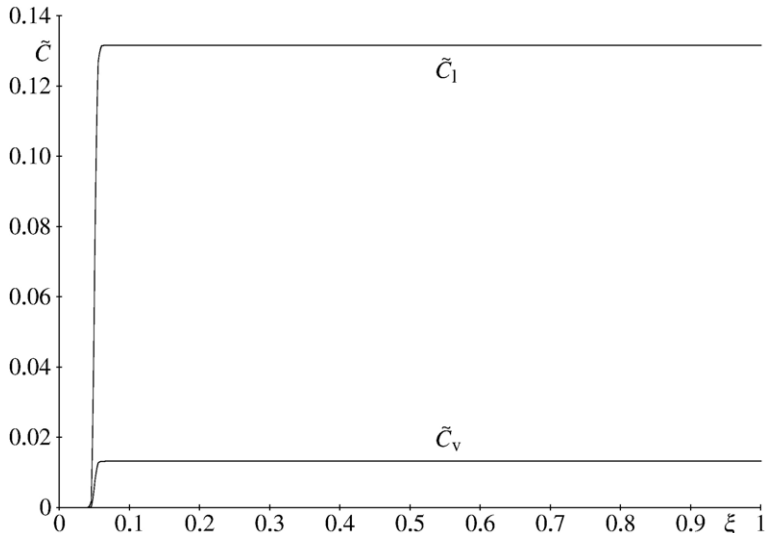


Fig. 7. Step-function profile.

Thus, at least boundary condition (32) should be satisfied. Substituting (35)–(37) in (32) and passing to the limit $M \rightarrow \infty$ yields

$$\left. \left(\beta(1+\varepsilon) \frac{\tau}{P} \frac{\partial \tilde{C}_v^{(0)}}{\partial \xi} + \frac{1-\beta\tilde{H}}{\tilde{H}} \tilde{C}_v^{(0)} \right) \right|_{\xi=\tau} = (1-\beta)\tilde{C}_{10} \quad (45)$$

for $0 < \tau \leq 1$. Eq. (38) with the boundary conditions (39) and (45) does constitute a well-posed problem. Thus, recalling (37), its solution gives the pointwise limiting behaviour of the solution of the original problem as $M \rightarrow \infty$. Moreover, the limit still satisfies the conservation of mass relation (31).

To see that the above deductions are consistent with the proposition that a boundary discontinuity occurs, one may substitute $\tilde{C}_v = \tilde{C}_v^{(0)} + \hat{C}_v(\eta, \tau) + O(1/M)$ and $\tilde{C} = \tilde{C}_v^{(0)} / \tilde{H} + \hat{C}_l(\eta, \tau) + O(1/M)$ where

$$\eta = -M\tilde{H}(\tau - \xi) \quad (46)$$

and

$$\hat{C}_v|_{\eta=-M\tilde{H}\tau} = \hat{C}_l|_{\eta=-M\tilde{H}\tau} = 0 \quad (47)$$

in (24)–(28). Subsequently, dividing (24) by M^2 , (25)–(28) by M , and passing to the limit $M \rightarrow \infty$, gives rise to

$$\frac{\partial^2 \hat{C}_v}{\partial \eta^2} = 0 \quad (48)$$

and

$$\frac{\partial \hat{C}_l}{\partial \eta} \Big|_{\eta=-\infty} = \frac{\beta(1+\varepsilon)}{\tilde{H}} \tau (\tilde{H}\hat{C}_l - \hat{C}_v) \quad (49)$$

for $\eta < 0$ and $0 < \tau \leq 1$, with

$$\frac{\partial \hat{C}_v}{\partial \eta} \Big|_{\eta=0} = \frac{\partial \hat{C}_v}{\partial \eta} \Big|_{\eta=0} = 0, \quad (50)$$

$$(\hat{C}_l - \beta\hat{C}_v) \Big|_{\eta=0} = (1-\beta)\tilde{C}_{10} + \frac{\beta\tilde{H}-1}{\tilde{H}} \tilde{C}_v^{(0)}(\tau, \tau) \quad (51)$$

and

$$\hat{C}_v|_{\eta=-\infty} = \hat{C}_l|_{\eta=-\infty} = 0 \quad (52)$$

for $0 < \tau \leq 1$. Although this is ostensibly an over-determined system, it admits a viable solution. From (48), (50) and (52) it follows that $\hat{C}_v \equiv 0$, whence from (49), (51) and (52) one may deduce that $\hat{C}_l(\eta, \tau) = \hat{C}_l(0, \tau) e^{\beta(1+\varepsilon)\tau\eta}$ where $\hat{C}_l(0, \tau) = \{(1-\beta)\tilde{C}_{10} + (\beta\tilde{H}-1)\tilde{C}_v^{(0)}(\tau, \tau)/\tilde{H}\}$. Transforming back to the original dimensionless variables, this gives

$$\tilde{C}_v(\xi, \tau) \simeq \tilde{C}_v^{(0)}(\xi, \tau)$$

and

$$\tilde{C}_l(\xi, \tau) \simeq \frac{\tilde{C}_v^{(0)}(\xi, \tau)}{\tilde{H}} + \left\{ (1-\beta)\tilde{C}_{10} + \frac{\beta\tilde{H}-1}{\tilde{H}} \tilde{C}_v^{(0)}(\tau, \tau) \right\} e^{-\beta(1+\varepsilon)M\tilde{H}\tau(\tau-\xi)}, \quad (53)$$

where $\tilde{C}_v^{(0)}$ is the solution of problem (38), (39), (45), as an approximation to the solution of problem (24)–(28) in the limit $M \rightarrow \infty$. The last term in (53) corresponds to a boundary-layer effect of width $O(1/M)$. By substitution of $\xi = \tau$ in (53), it is easily verifiable that this extra term leads to satisfaction of the boundary condition (28) at the expense of condition (27). In the limit $M \rightarrow \infty$, (53) exhibits the discontinuity

$$\tilde{C}_1(\xi, \tau) \approx \begin{cases} \frac{\tilde{C}_v^{(0)}(\xi, \tau)}{\tilde{H}} & \text{for } \xi < \tau \\ (1 - \beta)\tilde{C}_{10} + \beta\tilde{C}_v^{(0)}(\xi, \tau) & \text{for } \xi = \tau. \end{cases}$$

The described boundary-layer effect is visible in the numerically determined solution of problem (24)–(28) shown in Fig. 8. This shows the dimensionless concentration profiles at the end of the process, \tilde{C}_1 and \tilde{C}_v as functions of ξ for $\tau = 1$, computed with parameter values $\tilde{C}_{10} = 0.25$, $\beta = 0.5$, $M = 10^3$, $\tilde{H} = 1$, $\varepsilon = 0$ and $P = 1$.

When $P = \infty$ and $\beta > 1$, the first part of the above analysis is reproducible. Starting from (35) and (36) one may deduce that (37) holds and thereafter that $\tilde{C}_v^{(0)}$ satisfies (42) and (43). However, by the method of characteristics the only solution of this problem is $\tilde{C}_v^{(0)} = 0$. In combination with (37) this violates the conservation of mass condition (31). This paradox can be resolved by substituting $\hat{C}_v = M\hat{C}_v(\eta, \tau) + O(1)$ and $\hat{C}_1 = M\hat{C}_1(\eta, \tau) + O(1)$, where η is the boundary-layer variable (46) and where (47) holds, in problem (24)–(28). In such a case, it can be verified that the statement of overall conservation of mass transforms to

$$\int_{-M\tilde{H}\tau}^0 \{\beta\varepsilon\hat{C}_v(\eta, \tau) + \hat{C}_1(\eta, \tau)\} d\eta = (1 - \beta)\tilde{H}\tilde{C}_{10}\tau \quad (54)$$

for $0 \leq \tau \leq 1$. Dividing Eqs. (24) and (25) by M^2 , and, (26)–(28) by M , leaves the equations

$$\frac{\partial \hat{C}_v}{\partial \eta} = \frac{1 + \varepsilon}{\tilde{H}}\tau(\tilde{H}\hat{C}_1 - \hat{C}_v) \quad \text{and} \quad \frac{\partial \hat{C}_1}{\partial \eta} = \frac{\beta(1 + \varepsilon)}{\tilde{H}}\tau(\tilde{H}\hat{C}_1 - \hat{C}_v)$$

for $\eta < 0$ and $0 < \tau \leq 1$, together with the boundary conditions $(\hat{C}_1 - \beta\hat{C}_v)|_{\eta=0} = 0$ and (52) for $0 < \tau \leq 1$, in the limit $M \rightarrow \infty$. Although this is once more an over-specified problem, using the

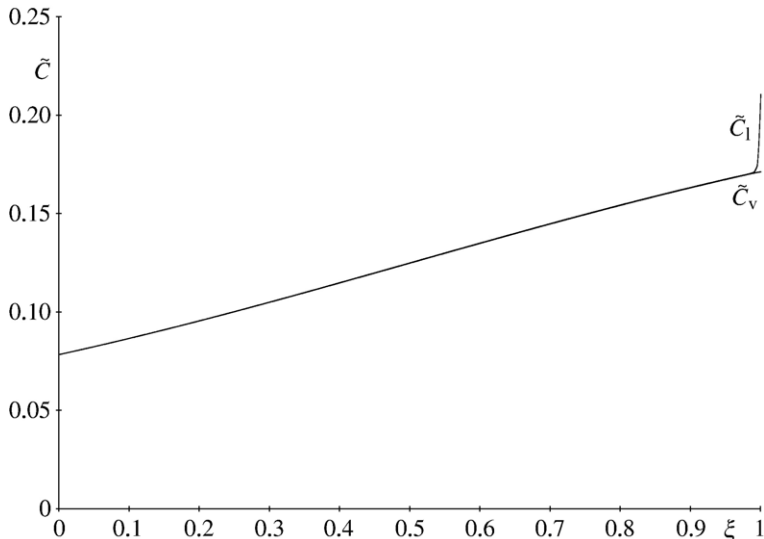


Fig. 8. Profile showing boundary layer.

theory of systems of first-order ordinary differential equations, it can be verified that it admits a solution of which the most general form is $\hat{C}_v(\eta, \tau) = \hat{C}_v(0, \tau)e^{(1+\varepsilon)(\beta\tilde{H}-1)\tau\eta/\tilde{H}}$ and $\hat{C}_1 \equiv \beta\hat{C}_v$. The unknown $\hat{C}_v(0, \tau)$ is determinable by substitution in the limit as $M \rightarrow \infty$ of the conservation of mass statement (54). Returning to the variables ξ and τ this gives

$$\tilde{C}_v(\xi, \tau) \simeq \frac{1-\beta}{\beta} (\beta\tilde{H}-1) M \tilde{C}_{10} \tau^2 e^{-(1+\varepsilon)(\beta\tilde{H}-1)M\tau(\tau-\xi)} \quad (55)$$

and

$$\tilde{C}_1(\xi, \tau) \simeq (1-\beta)(\beta\tilde{H}-1) M \tilde{C}_{10} \tau^2 e^{-(1+\varepsilon)(\beta\tilde{H}-1)M\tau(\tau-\xi)}. \quad (56)$$

Thus, in the case $P = \infty$ and $\beta\tilde{H} > 1$ one obtains an infinite boundary-layer effect. The width of the boundary-layer is $O(1/M)$, but, at the same time, its height grows as $O(M)$ to preserve conservation of mass. This effect is clearly visible in the numerically computed solution displayed in Fig. 9. This shows the dimensionless concentration profiles \tilde{C}_1 and \tilde{C}_v for $\tau = 1$ as functions of ξ , computed with the parameter values $\tilde{C}_{10} = 0.25$, $\beta = 0.5$, $M = 10$, $\tilde{H} = 100$, $\varepsilon = 0$ and $P = 10^{99}$.

Formulae (55) and (56) imply that $\tilde{C}_1(1, 1) \sim (1-\beta)(\beta\tilde{H}-1)M\tilde{C}_{10}$ and $\tilde{C}_v(1, 1) \sim \tilde{C}_1(1, 1)/\beta$ as $M \rightarrow \infty$. Hence, for any fixed combination of parameter values $0 < \tilde{C}_{10} < 1$, $0 < \beta < 1$, $\tilde{H} > 1/\beta$, $\varepsilon \geq 0$ and $P = \infty$, as the Merkle number progressively increases one will encounter the situation that the constraint (29) or (30) is violated. In fact, if M is sufficiently large, both constraints will fail. By extrapolation, for any \tilde{C}_{10} , β , \tilde{H} and ε as described, this conclusion still holds for a large enough Péclet number P .

Case 4 ($\tilde{H} \rightarrow \infty$). The analysis of the limiting situation as $\tilde{H} \rightarrow \infty$ can be carried out similarly to the previous case.

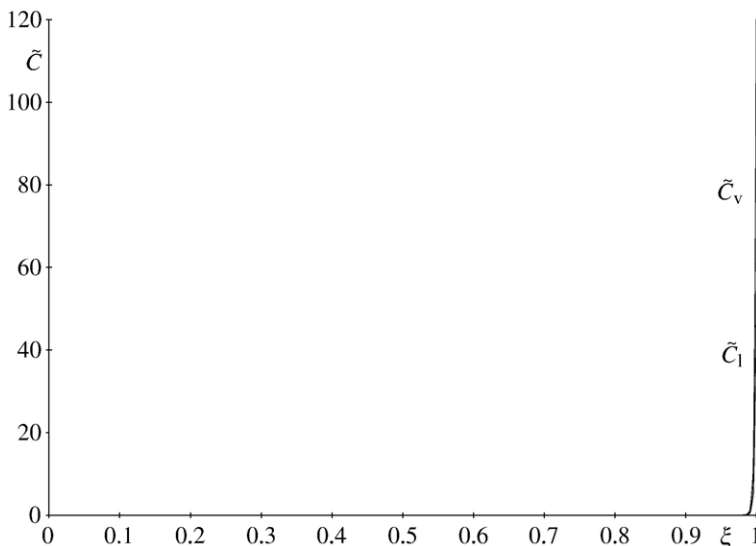


Fig. 9. Profile showing infinite boundary layer.

Without going into details, if $\varepsilon > 0$ and $P < \infty$ then substituting

$$\tilde{C}_v = \tilde{C}_v^{(0)}(\xi, \tau) + O(1/\tilde{H})$$

and

$$\tilde{C}_l = \tilde{C}_l^{(0)}(\xi, \tau) + \tilde{C}_l^{(1)}(\xi, \tau)/\tilde{H} + O\left(1/\tilde{H}^2\right)$$

in (24)–(26) and the ‘conservation of mass’ boundary condition (32) one finds that

$$\tilde{C}_l^{(0)} \equiv 0 \quad \text{and} \quad \tilde{C}_l^{(1)} \equiv \tilde{C}_v^{(0)}, \quad (57)$$

where $\tilde{C}_v^{(0)}$ is the solution of Eq. (33) for $0 < \xi < \tau \leq 1$, satisfying the boundary conditions (39) and

$$\left. \left(\beta(1 + \varepsilon) \frac{\tau}{P} \frac{\partial \tilde{C}_v^{(0)}}{\partial \xi} - \beta \tilde{C}_v^{(0)} \right) \right|_{\xi=\tau} = (1 - \beta) \tilde{C}_{l0}$$

for $0 < \tau \leq 1$. Subsequently substituting

$$\tilde{C}_v = \tilde{C}_v^{(0)} + \hat{C}_v(\eta, \tau) + O(1/\tilde{H}) \quad \text{and} \quad \tilde{C}_l = \hat{C}_l(\eta, \tau) + O(1/\tilde{H})$$

where η is defined by (46) and where (47) holds, into problem (24)–(28), gives

$$\hat{C}_v \equiv 0 \quad \text{and} \quad \hat{C}_l(\eta, \tau) = \left\{ \beta \tilde{C}_v^{(0)}(\tau, \tau) + (1 - \beta) \tilde{C}_{l0} \right\} e^{\beta(1+\varepsilon)\tau\eta}.$$

Thus there is again a boundary-layer effect such that (28) is fulfilled at the expense of (27).

When $P = \infty$, the situation arises that an infinite boundary-layer effect comes into play. One finds that

$$\tilde{C}_v(\xi, \tau) \simeq (1 - \beta) M \tilde{H} \tilde{C}_{l0} \tau^2 e^{-\beta(1+\varepsilon)M\tilde{H}\tau(\tau-\xi)}$$

and

$$\tilde{C}_l(\xi, \tau) \simeq \beta(1 - \beta) M \tilde{H} \tilde{C}_{l0} \tau^2 e^{-\beta(1+\varepsilon)M\tilde{H}\tau(\tau-\xi)}.$$

The exceptional situation when $\tilde{H} \rightarrow \infty$ is exhibited in the event that $\varepsilon = 0$ and $P < \infty$. In this situation, it can be determined that substitution of $\tilde{C}_v = \tilde{H} \tilde{C}_v^{(0)}(\xi, \tau) + O(1)$ and $\tilde{C}_l = \tilde{H} \tilde{C}_l^{(0)}(\xi, \tau) + \tilde{C}_l^{(1)}(\xi, \tau) + O(1/\tilde{H})$ into (24)–(26) and (32) leads to the conclusion that (57) holds, where $\tilde{C}_v^{(0)}$ is a solution of

$$0 = \frac{\tau}{P} \frac{\partial^2 \tilde{C}_v^{(0)}}{\partial \xi^2} - \frac{\partial \tilde{C}_v^{(0)}}{\partial \xi}$$

for $0 < \xi < \tau \leq 1$, satisfying (39) and

$$\left. \left(\frac{\tau}{P} \frac{\partial \tilde{C}_v^{(0)}}{\partial \xi} - \tilde{C}_v^{(0)} \right) \right|_{\xi=\tau} = 0$$

for $0 < \tau \leq 1$. Thus $\tilde{C}_v^{(0)}$ takes the form $\tilde{C}_v^{(0)}(\xi, \tau) = \tilde{C}_v^{(0)}(\tau, \tau) e^{-P(\tau-\xi)/\tau}$. Thereafter, substituting $\tilde{C}_v = \tilde{H} \tilde{C}_v^{(0)} + \tilde{H} \hat{C}_v(\eta, \tau) + O(1)$ and $\tilde{C}_l = \tilde{C}_v^{(0)} + \tilde{H} \hat{C}_l(\eta, \tau) + O(1)$ with η defined by (46) and with (47) holding, into problem (24)–(28) leads to (48) and

$$\frac{\partial \hat{C}_l}{\partial \eta} = \beta \tau \hat{C}_l$$

for $\eta < 0$ and $0 < \tau \leq 1$, and to the boundary condition (50), $(\hat{C}_1 - \beta \hat{C}_v)|_{\eta=0} = \beta \tilde{C}_v^{(0)}(\tau, \tau)$ and (52) for $0 < \tau \leq 1$. This gives the formulae $\hat{C}_v \equiv 0$ and $\hat{C}_1(\eta, \tau) = \beta \tilde{C}_v^{(0)}(\tau, \tau) e^{\beta \tau \eta}$. Transforming back to the original variables then yields

$$\tilde{C}_v(\xi, \tau) \approx \tilde{H} \tilde{C}_v^{(0)}(\tau, \tau) e^{-P(\tau-\xi)/\tau} \quad (58)$$

and

$$\tilde{C}_1(\xi, \tau) \approx \tilde{C}_v^{(0)}(\tau, \tau) \left\{ e^{-P(\tau-\xi)/\tau} + \beta \tilde{H} e^{-\beta M \tilde{H} \tau (\tau-\xi)} \right\}. \quad (59)$$

The unknown $\tilde{C}_v^{(0)}(\tau, \tau)$ is finally determined by the mass-balance relation (31). Substituting (58) and (59) into (31) and then letting $\tilde{H} \rightarrow \infty$ gives

$$\tilde{C}_v^{(0)}(\tau, \tau) = \frac{(1 - \beta) P M \tilde{C}_{10} \tau^2}{P + M(1 - e^{-P}) \tau^2}.$$

Thus in this situation as $\tilde{H} \rightarrow \infty$ the function \tilde{C}_v blows up everywhere, while \tilde{C}_1 exhibits an infinite boundary-layer. This is confirmed by Fig. 10. This shows the results of a numerical computation, similar to those previously presented, with the parameter values $\tilde{C}_{10} = 0.25$, $\beta = 0.5$, $M = 0.1$, $\tilde{H} = 10^4$, $\varepsilon = 0$ and $P = 1$.

For $\varepsilon = 0$, the limiting behaviour in the cases $P = \infty$ and $P < \infty$ can be combined to deduce that $\tilde{C}_v(1, 1) \sim (1 - \beta) M \tilde{H} \tilde{C}_{10} / \{1 + M(1 - e^{-P})/P\}$ and $\tilde{C}_1(1, 1) \sim \beta \tilde{C}_v(1, 1)$ as $\tilde{H} \leq \infty$. Thus, with fixed parameter values $0 < \tilde{C}_{10} < 1$, $0 < \beta < 1$, $M > 0$, $\varepsilon \geq 0$ and $0 < P \leq \infty$, the constraint (29) will necessarily fail if the transformed Henry number becomes exceedingly large. On the other hand, the constraint (30) may or may not fail dependent upon the exact values of \tilde{C}_{10} , β , M and P .

6. Quantitative significance of diffusion/dispersion

Realistic ranges of the physical property values associated with steam stripping of the unsaturated zone of soils contaminated with VOCs in practice are displayed in Table 1. These

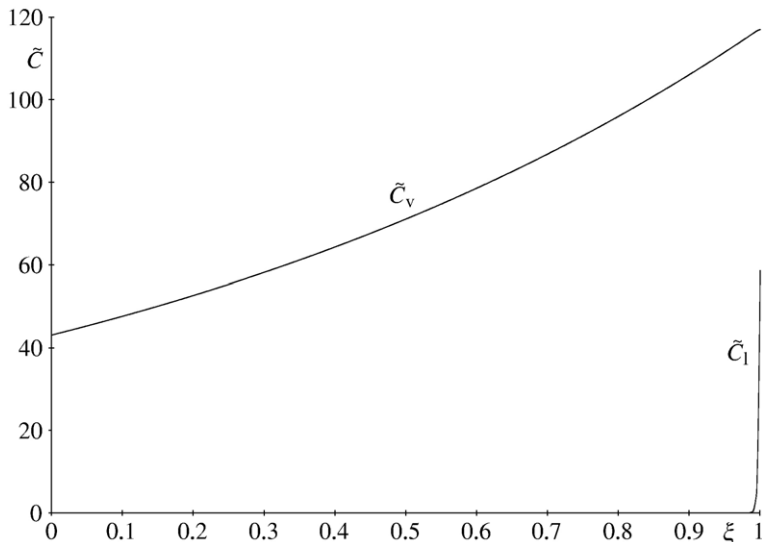


Fig. 10. Profile showing blow up.

Table 1

Typical values of physical properties

$10^{-12} \text{ m}^2 < \kappa < 10^{-8} \text{ m}^2$
$10^4 \text{ Pa} < p_{\text{in}} - p_0 < 2 \times 10^4 \text{ Pa}$
$0.01 < \phi S_{lc} < 0.08$
$10^{-5} \text{ m}^2 \text{ s}^{-1} < D < 10^{-4} \text{ m}^2 \text{ s}^{-1}$
$0.1 \text{ m} < L < 10 \text{ m}$
$10^{-3} \text{ s}^{-1} < g_i < 0.1 \text{ s}^{-1}$
$10^6 \text{ J m}^{-3} \text{ K}^{-1} < \rho_s c_{ps} < 2 \times 10^6 \text{ J m}^{-3} \text{ K}^{-1}$
$0.1 < H < 100$
$H_{\text{lat}} = 2 \times 10^6 \text{ J kg}^{-1}$
$\rho_v = 1 \text{ kg m}^{-3}$
$\rho_l = 10^3 \text{ kg m}^{-3}$
$T_{\text{sat}} - T_0 = 100 \text{ K}$
$v_v = 2 \times 10^{-5} \text{ m}^2 \text{ s}^{-1}$

values yield a spread of the Merkel number from 10^{-6} to 2×10^4 and a range for the transformed Henry number \tilde{H} of 100 to 10^5 .

Using the numerical scheme described in the Appendix, computations were carried out to evaluate the significance of diffusion/dispersion with the representative values $\tilde{C}_{10}=0.25$, $\beta=0.5$ and $\varepsilon=0$, for $M=10^{-6}, 10^{-5}, 10^{-4}, \dots, 10^4$, $\tilde{H}=100, 10^3, 10^4, 10^5$, and, $P=0.1, 1, 10, 100, 10^{99}$. The value of $P=10^{99}$ corresponds to negligible diffusion/dispersion. It transpires that this range of parameter values of M , \tilde{H} and P is such that limiting behaviour phenomena as described in the previous section are encountered.

It emerges from the computations that when $M\tilde{H} \leq 0.1$, irrespective of the value of P , the dimensionless liquid concentration \tilde{C}_l at the end of the process does not drop below 95% of the uniform profile $(1-\beta)\tilde{C}_{10}$. Thus this can be considered as corresponding with the theoretical limits $M \rightarrow 0$ and $\tilde{H} \rightarrow 0$ described in the previous section. In practice this would indicate that when $M\tilde{H} \leq 0.1$, steam stripping will have little effect on removing contaminants.

In contrast, when $M\tilde{H} \geq 100$, irrespective of the value of P , the computed profiles \tilde{C}_l and \tilde{C}_v do not satisfy the physical constraints on the validity of the model (29) and (30) at the end of the process. In the light of the analysis of the previous section, this quantifies how for $\beta\tilde{H} > 1$, taking M too large leads to a physically unrealistic model. Alternatively, for a fixed Merkel number it indicates how a sufficiently large transformed Henry number will lead to an unacceptable result. Significantly, in none of the cases examined does (30) fail without (29) failing as well. It is to be recalled that failure of (29) implies that the solubility limit is exceeded, and for such a situation, additional modelling considerations are appropriate.

For those values of M and \tilde{H} that yield solutions satisfying the modelling constraints, the executed computations have been further analyzed to evaluate the quantitative importance of diffusion/dispersion. The criterion adopted is the following. Diffusion/dispersion has a significant effect if and only if it results in a drop of the contaminant concentration in vapour phase \tilde{C}_v at the monitoring point at the end of the process of at least 10% when compared to the situation with no diffusion/dispersion. With this quantitative criterion, it appears that diffusion/dispersion does not have a significant effect. This is notwithstanding that diffusion/dispersion does influence the profile of contaminant concentration in vapour phase behind the front. See Fig. 5 for a typical illustration of what occurs.

7. Conclusions

The present paper addresses steam stripping of the unsaturated zone of sub-soils that are contaminated with VOCs. Attention is focussed on the start-up phase. During this phase, steam enters the porous medium, condenses at the steam front, and air initially present in the porous medium is driven out. The contaminant is evaporated and transported behind the front towards it.

The propagation of the steam front has been modelled. To determine its position, the vapour flow to the front using Darcy's law, and an energy balance at the front have been employed. In contrast to the earlier analyses in (Brouwers and Li, 1994, 1995), in the present analysis, saturation of the vapour phase has been taken into account, leading to the dimensionless factor ε . It is demonstrated that as a function of time t the steam-front position follows $\lambda\sqrt{At}/(1+\varepsilon)$, where λ and A are further dimensionless process-dependent parameters. The value of λ , $0 < \lambda < 1$, follows from an algebraic equation. In the limit that heat loss ahead of the front is negligible, λ approaches its upper bound.

Building on the model of the steam-front propagation, the transport of contaminant behind the front has been considered. A non-equilibrium model that involves transport of the contaminant dissolved in the liquid water phase to the vapour phase has been proposed. This model accounts for advective and diffusive/dispersive transport of contaminant in the vapour phase. A careful consideration of contaminant mass balances at the steam front for both the vapour and liquid phases, (17) and (19), yields the necessary boundary conditions (18) and (20), to complete the governing partial differential equations (14) and (15) and the boundary condition (16).

The resulting complete moving-boundary problem has been transformed and made dimensionless. Besides the measure ε of saturation in the vapour phase, the final system, (24)–(28), contains five dimensionless parameters: the Péclet number P which denotes the ratio of advective to diffusive transport, the Merkel number M which represents the ratio of the mass-transfer rate to advective transport, the modified Henry's law coefficient \tilde{H} , the amount β of condensed water in relation to the total amount of water, and, \tilde{C}_{10} which represents the initial concentration of the contaminant in the liquid phase. A suitable discretization has been put forward in order to solve the system numerically. This leads to a scheme that can be solved by a standard algorithm.

With fixed values of the system parameters, numerical solutions have been computed and the accuracy of the algorithm examined. It has been demonstrated that the computational results are consistent with those of Brouwers and Li (1995). Furthermore, it has been shown that the introduction of the additional system parameters ε and P over and above those found in the earlier works (Brouwers and Li, 1994, 1995) has the qualitative effect on the start-up phase of the transport of contaminant that one would expect on physical grounds.

With representative values of \tilde{C}_{10} , β and ε , and for the range of parameter values M , \tilde{H} and P one would encounter based on physical data, computations have been carried out to investigate the quantitative effect of these parameters. It turns out that a variety of phenomena can be observed. At one extreme, effectively no contaminant is removed. At the other extreme, the solubility limit can be exceeded. These observations are borne out by an asymptotic analysis of the limiting behaviour with respect to the parameters M and \tilde{H} .

Last but not least, for those situations in which the model remains valid, the quantitative effect of diffusion/dispersion has been analyzed. It has been found that this phenomenon actually

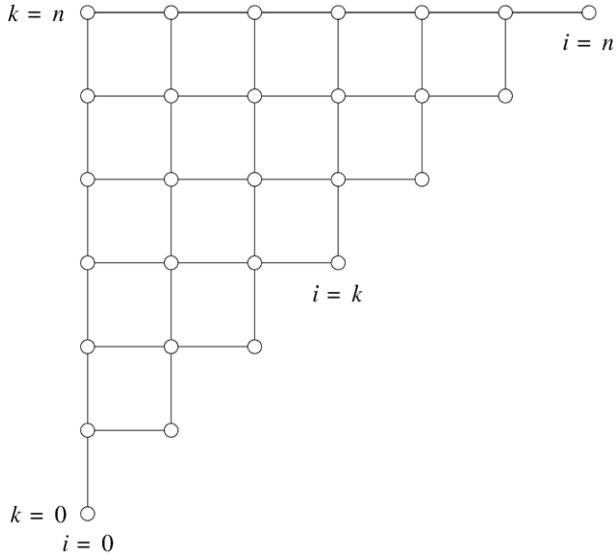


Fig. A.1. Discretization grid.

has little quantitative influence on the removal of contaminants during the start-up phase of steam stripping of the unsaturated zone of sub-soils.

Appendix A. Numerical solution

This appendix describes a numerical scheme for solving the boundary-value problem (24)–(28), and its validation.

A uniform grid in ξ and τ has been chosen so that the dimensionless-time interval $0 \leq \tau \leq 1$ is divided into n equal steps of size $h = 1/n$, and at any dimensionless time $\tau_k = kh$ with $1 \leq k \leq n$ the dimensionless-spatial interval $0 \leq \xi \leq \tau_k$ is divided into k steps of size h . The mesh points are then

$$(\xi_i, \tau_k) = (ih, kh)$$

for $i = 0, 1, \dots, k$ and $k = 0, 1, \dots, n$ (Fig. A.1). Denote the unknowns \tilde{C}_v and \tilde{C}_l in the mesh point (ξ_i, τ_k) by $C_v^{i,k}$ and $C_l^{i,k}$, respectively.

On the aforementioned grid, Eq. (24) can be discretized by using a fully implicit scheme for the dimensionless-time derivative and an upwind scheme for the advective term as

$$\frac{\varepsilon}{1 + \varepsilon} \frac{C_v^{i,k} - C_v^{i,k-1}}{h} = \frac{\tau_k}{P} \frac{C_v^{i+1,k} - 2C_v^{i,k} + C_v^{i-1,k}}{h^2} - \frac{C_v^{i,k} - C_v^{i-1,k}}{h} + M\tau_k (\tilde{H}C_l^{i,k} - C_v^{i,k}) \quad (\text{A.1})$$

for $1 \leq i \leq k-1$ and $1 \leq k \leq n$. While Eq. (25) can be similarly discretized with a fully implicit scheme as

$$\frac{C_l^{i,k} - C_l^{i,k-1}}{h} = -\beta(1 + \varepsilon)M\tau_k (\tilde{H}C_l^{i,k} - C_v^{i,k}) \quad (\text{A.2})$$

for $0 \leq i \leq k-1$ and $1 \leq k \leq n$. A corresponding straightforward discretization of the boundary conditions (26) and (27) leads to

$$C_v^{0,k} - \frac{\tau_k}{P} \frac{C_v^{1,k} - C_v^{0,k}}{h} = 0 \quad (\text{A.3})$$

and

$$C_v^{k,k} - C_v^{k-1,k} = 0 \quad (\text{A.4})$$

for $1 \leq k \leq n$, respectively. The condition (28) can be represented by

$$C_1^{k,k} - \beta C_v^{k,k} = (1 - \beta) \tilde{C}_{10} \quad (\text{A.5})$$

for $0 \leq k \leq n$. The local truncation error of this numerical scheme is $O(h)$.

Eqs. (A.1)–(A.5) provide an algorithm for computing $C_v^{i,k}$ and $C_1^{i,k}$ for all $0 \leq i \leq k \leq n$. The key is that Eq. (A.2) may be rewritten as

$$C_l^{i,k} = \frac{C_l^{i,k-1} + \beta(1 + \varepsilon)M\tau_k h C_v^{i,k}}{1 + \beta(1 + \varepsilon)M\tilde{H}\tau_k h} \quad (\text{A.6})$$

for $0 \leq i \leq k-1$ and $1 \leq k \leq n$.

Substituting Eq. (A.6) into Eq. (A.1) and combining with Eqs. (A.3) and (A.4) leads to the system of equations

$$\begin{cases} b^{0,k} C_v^{0,k} + c^{0,k} C_v^{1,k} = 0 \\ a^{i,k} C_v^{i-1,k} + b^{i,k} C_v^{i,k} + c^{i,k} C_v^{i+1,k} = f^{i,k} & \text{for } 1 \leq i \leq k-1 \\ -C_v^{k-1,k} + C_v^{k,k} = 0, \end{cases} \quad (\text{A.7})$$

where

$$b^{0,k} = 1 + \frac{\tau_k}{Ph}, \quad c^{0,k} = -\frac{\tau_k}{Ph}, \quad (\text{A.8})$$

$$a^{i,k} = -1 - \frac{\tau_k}{Ph}, \quad (\text{A.9})$$

$$b^{i,k} = \frac{1 + 2\varepsilon}{1 + \varepsilon} + \frac{2\tau_k}{Ph} + \frac{M\tau_k h}{1 + \beta(1 + \varepsilon)M\tilde{H}\tau_k h}, \quad (\text{A.10})$$

$$c^{i,k} = -\frac{\tau_k}{Ph} \quad (\text{A.11})$$

and

$$f^{i,k} = \frac{\varepsilon}{1 + \varepsilon} C_v^{i,k-1} + \frac{M\tilde{H}\tau_k h}{1 + \beta(1 + \varepsilon)M\tilde{H}\tau_k h} C_1^{i,k-1} \quad (\text{A.12})$$

for $1 \leq i \leq k - 1$, or alternatively, where

$$b^{0,k} = 1 + \frac{Ph}{\tau_k}, \quad c^{0,k} = -1, \quad (\text{A.13})$$

$$a^{i,k} = -1 - \frac{Ph}{\tau_k}, \quad (\text{A.14})$$

$$b^{i,k} = 2 + \frac{(1+2\varepsilon)Ph}{(1+\varepsilon)\tau_k} + \frac{MPh^2}{1+\beta(1+\varepsilon)M\tilde{H}\tau_k h}, \quad (\text{A.15})$$

$$c^{i,k} = -1 \quad (\text{A.16})$$

and

$$f^{i,k} = \frac{\varepsilon Ph}{(1+\varepsilon)\tau_k} C_v^{i,k-1} + \frac{M\tilde{H}Ph^2}{1+\beta(1+\varepsilon)M\tilde{H}\tau_k h} C_1^{i,k-1} \quad (\text{A.17})$$

for $1 \leq i \leq k - 1$.

Using the above formulation, the solution may be computed at successive dimensionless times τ_k for $k=0, 1, 2, \dots, n$ by first determining $C_v^{i,k}$ for $0 \leq i \leq k$ and thereafter $C_1^{i,k}$ for $0 \leq i \leq k$. To start, combining conditions (26) and (27) formally yields $\tilde{C}_v|_{\xi=\tau=0}=0$. So, one can take

$$C_v^{0,0} = 0.$$

Next, combining Eqs. (A.3) and (A.4) for $k=1$ leads to

$$C_v^{0,1} = C_1^{1,1} = 0.$$

So, $C_v^{0,1}$ and $C_1^{1,1}$ are also known. For $k > 1$, once $C_v^{i,k-1}$ and $C_1^{i,k-1}$ are known for $0 \leq i \leq k - 1$, (A.7) represents a tri-diagonal system of equations in the unknowns $C_v^{i,k}$ for $0 \leq i \leq k$. These unknowns can subsequently be computed using a standard algorithm which is commonly attributed to Thomas (Remson et al., 1971; Press et al., 1986). In coding, the formulation (A.8)–(A.12) has been used when $\tau_k \leq Ph$ and the formulation (A.13)–(A.17) when $\tau_k > Ph$, as a precaution for maintaining the stability of the computations. Once $C_v^{i,k}$ is known for all $0 \leq i \leq k$ and any $k \geq 0$, Eq. (A.6) gives $C_1^{i,k}$ for $0 \leq i \leq k - 1$ and Eq. (A.5) gives $C_1^{k,k}$. Thus $C_v^{i,k}$ and $C_1^{i,k}$ can be computed in succession for all $0 \leq i \leq k \leq n$.

Except for one detail, the numerical scheme derived above is equivalent to that of Brouwers and Li (1995) for the case $\varepsilon=0$ and $P=\infty$. The exceptional detail is that in the earlier code the discretization (A.1) with $\varepsilon=0$, $P=\infty$ and $i=k$ was employed in the place of (A.4). This is related to the fact that when $P=\infty$, the boundary condition (27) is satisfied automatically, so the imposition of (A.4) is inappropriate. On the other hand, since the second-order term in Eq. (24) disappears, the discretization (A.1) with $i=k$ can be applied without involving a fictive unknown $C_v^{k+1,k}$.

The accuracy of the numerical scheme has been investigated in the following way. With fixed parameter values $\tilde{C}_{10}=0.25$, $\beta=0.5$, $M=0.1$, $\tilde{H}=40$, $\varepsilon=0.1$ and $P=1$, computations were carried out with values of $n=10, 20, 50, 100, 200, 500, 1000, 2000, 5000, 10000, 20000, 50000$ and 100000 . See Fig. 6 for $C_1^{i,n}$ and $C_v^{i,n}$ as functions of ξ_i for $i=0, 1, \dots, n$ computed with the largest number of grid points. All profiles are such that the largest computed dimensionless

concentration is consistently $C_v^{n,n}$. Subsequently, assuming that the computed value $C_v^{n,n}$ can be developed as a Taylor series in $h=1/n$, as many coefficients in this series as could be determined using the data for the stated values of n were computed. On the basis of this expansion, the value C^* that would result from passage to the limit $h \rightarrow 0$ was estimated. Hereafter, a plot on log–log scale was made of the estimated relative error $|C_v^{n,n} - C^*|/C^*$ versus n . As shown as the representative case in Fig. A.2, the points in this plot lie on a straight line with gradient –1. This demonstrates that the convergence of the numerical method is $O(h)$, consistent with the local truncation error of the discretization.

Conduction of the above experiment with the code described in Brouwers and Li (1995) with values $\tilde{C}_{10}=0.25$, $\beta=0.5$, $M=0.1$ and $\tilde{H}=400$ ($\varepsilon=0$ and $P=\infty$), which lead to a very sharp profile, gave rise to the plot shown as the worst case in Fig. A.2. This indicates that in this extreme case, $n=20\,000$ is required to obtain a relative error of less than 1%, and $n=200\,000$ to obtain a relative error of less than 0.1%. On the basis of this information, all computations described elsewhere in this paper were performed with $n=100\,000$. This is notwithstanding that from the representative case, it could be deduced that a value of $n=500$ is more than adequate to compute the solution with a relative error of 1%, while $n=5000$ is amply sufficient for a relative error of 0.1%.

To complete the validation of the numerical scheme presented above, it was employed to reproduce the computations in Brouwers and Li (1995). For this purpose values $\varepsilon=0$ and $P=10^{99}$ were chosen to emulate the effect of neglecting the saturation in vapour phase ($\varepsilon=0$) and diffusion/dispersion ($P=\infty$). The results of the computations with $n=100\,000$ and

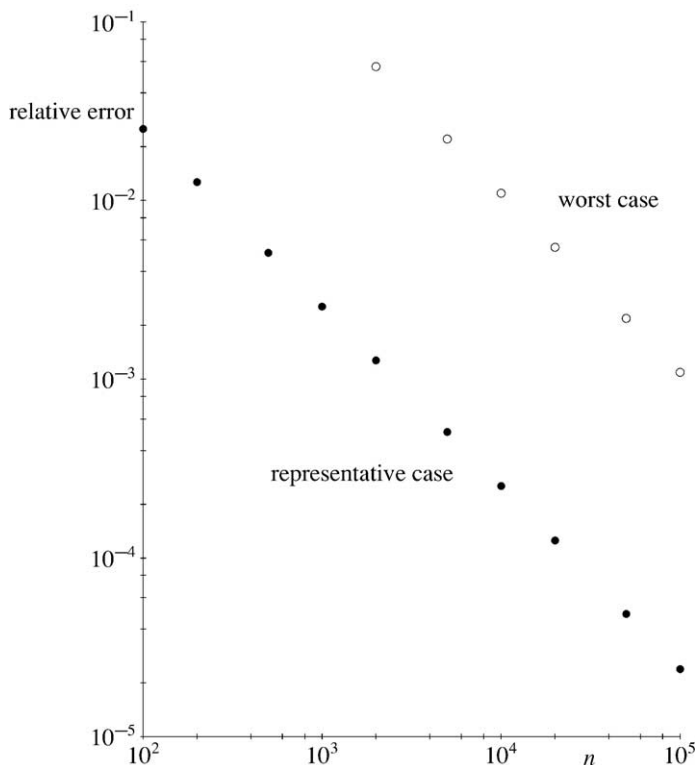


Fig. A.2. Relative numerical error versus number of discretization steps.

parameter values otherwise as used by [Brouwers and Li \(1995\)](#) are not visually distinguishable from their computations.

References

- Bear, J., 1979. *Hydraulics of Groundwater*. McGraw-Hill, New York.
- Brouwers, H.J.H., 1996. An experimental study of constant-pressure steam injection and transient condensing flow in an air-saturated porous medium. *ASME J. Heat Transfer* 118, 449–454.
- Brouwers, H.J.H., 1999. Transport models for desorption from natural soils packed in flushed columns. *Water Resour. Res.* 35, 1771–1780.
- Brouwers, H.J.H., Augustijn, D.C.M., 2001. Analytical model for removal of a uniformly distributed single-component NAPL under nonequilibrium conditions. *Groundwater Monit. and Remediat.* 21, 162–171.
- Brouwers, H.J.H., Li, S., 1994. An analysis of constant pressure steam injection in an unsaturated porous medium. In: Hewitt, G.F. (Ed.), *Proceedings of the Tenth International Heat Transfer Conference, Heat Transfer vol. 5*. Institute of Chemical Engineers, Rugby, UK, pp. 219–224.
- Brouwers, H.J.H., Li, S., 1995. Steam stripping of contaminated unsaturated zone of subsoils: Theoretical model of start-up phase. *Water Resour. Res.* 31, 2253–2261.
- Gilding, B.H., Li, S., 1997. The parameter dependence of the coefficient in a model for constant-pressure steam injection in soil. *Math. Models Methods in Appl. Sci.* 7, 593–612.
- van der Ham, A.G.J., Brouwers, H.J.H., 1998. Modeling and experimental investigation of transient, nonequilibrium mass transfer during steam stripping of a nonaqueous phase liquid in unsaturated porous media. *Water Resour. Res.* 34, 47–54.
- Press, W.H., Flannery, B.P., Teukolsky, S.A., Vetterling, W.T., 1986. *Numerical Recipes*. Cambridge University Press, Cambridge, UK.
- Remson, I., Hornberger, G.M., Molz, F.J., 1971. *Numerical Methods in Subsurface Hydrology with an Introduction to the Finite Element Method*. Wiley-Interscience, New York.
- Russo, G., 1998. A remark on “The parameter dependence of the coefficient in a model for constant pressure steam injection in soil”. *Math. Models Methods in Appl. Sci.* 8, 1317–1321.